Hydrodynamic interactions between three closely-spaced Vertical Axis Tidal Turbines

Stefania Zanforlin*, Ferdinando Burchi, Niccolò Bitossi

Department of Energy, Systems, Territory and Constructions Engineering, University of Pisa, l.go L. Lazzarino, 56122 Pisa, Italy

Abstract

A CFD analysis of the hydrodynamic interactions between three vertical axis tidal turbines set in close proximity is performed for two layout: side-by-side and triangular. The following key mechanisms are found to determine a power increasing with respect to isolated turbines: (1) turbine blockage that entails flow acceleration outside of the turbines and inside the aisles between adjacent turbines; (2) more favorable direction of the flow approaching the blade during upwind; (3) wake contraction, that increases torque generation during downwind. Blockage is responsible for a moderate performance increasing exhibited by the triangular layout. Change in the direction of the flow approaching the blades and wake contraction only occur for side-by-side layout, and lead to a significant increasing of efficiency. The side-by-side layout allows a wider range of flow directions that make possible a power gain, and thus it could be adoptable for tidal currents characterized by an incomplete inversion of the current direction. The behaviors of the two arrangements are compared for a real case located in the Strait of Messina.

Keywords: vertical axis tidal turbine; wake; blockage; hydrodynamic interactions.

1. Introduction

Tidal current energy has been identified as one of the most promising renewable resources in the European Union. It has important advantages, such as predictability and invisibility with respect to the principal competing, such as wind and wave power, offering important attractions to power distribution and supply companies.

---

* Corresponding author. Tel.: +39-050-2217145; fax: +39-050-2217150.
  E-mail address: s.zanforlin@ing.unipi.it

Horizontal or vertical axis turbines can be used. The main advantages of vertical axis tidal turbines (VATT) are the ability to keep the electric generator out of the water, by using floating platforms as support structure, and to be omnidirectional, without the need for any active yaw device. On the other hand, VATT are penalized by a low efficiency compared to horizontal axis tidal turbines (HATT) and by self-starting issues. Then, it is essential to increase the efficiency of the overall arrangement as a well as the power density. To increase the power produced in a given area of sea it would be convenient to place a farm of high aspect-ratio (AR > 2) turbines arranged as close as possible, compatibly with the negative effects of wake interactions. Numerical studies aimed to optimize the arrangement of HATT or VATT farm or rows proved that the local blockage mechanism (the acceleration of flow between two adjacent turbines) can be exploited to increase the energy production by dislocating the turbines belonging to two consecutive rows in staggered arrangements [1, 2].

Experimental studies on arrangements of vertical axis turbine are few and mainly focused to wind farm. The most important study is the experimental campaign carried out by Dabiri and his team [3-5] who measured a performance increasing by placing the turbines not only in staggered rows but also two-by-two in close proximity and counter-rotating. However, the theoretical models implemented are focused on the evolution of the energy content of the field and on the energy recovery in the wakes, while the turbines are treated as bluff bodies in which a negative source of momentum is superimposed to take into account the power extracted. The interference between two VATT, counter-rotating or co-rotating, has been investigated experimentally and numerically by Li and Çalişal [6], yet the model, based on the vortex method, does not allow to identify the physical phenomena that can determine a performance increasing or a detriment depending on the relative arrangement (angular position and distance) of the rotors. Later, the vortex method has been adopted by Feng et al. [7] to predict the behaviour of two counter-rotating closely spaced wind turbines versus wind direction. Despite a large number of Unsteady Reynolds Averaged Navier-Stokes (URANS) CFD investigations of single vertical axis, wind or tidal, turbines, there are still few analyses on wake interferences in two or more turbine arrangements. A first attempt to investigate the interactions between arrangements of closely spaced vertical axis wind turbines by means of CFD was done by Giorgetti et al. [8] who focused on the wake re-energisation due to wake contraction. Recently, Zanforlin and Nishino [9] performed a comprehensive set of 2D URANS simulations of flow around a pair of counter-rotating vertical-axis wind turbines with various gaps between the rotors, tip-speed-ratios and wind directions. They observed that the mechanisms playing an important role in performance increasing respect to an isolated turbine are the improving in the direction of the flow approaching the blade in upwind and the increasing of the velocity magnitude in downwind due to wake contraction. Starting from these findings, we analyse the hydrodynamic interactions responsible for power rising in two layout of 3 VATT: side-by-side and equilateral triangle. Then we show the predicted power gain (or loss) with respect to isolated turbines versus the current direction. Finally we predict the geographical orientation of the two layout that maximize the energy output gain during 28 days for a real case in the Strait of Messina.

2. Model set-up and validation

The validation of the computational model is done for a small 3-blade H-Darrieus water turbine tested by Maître et al. [10] in a hydrodynamic tunnel. Turbine diameter (D) and blade length (H) are 175mm, thus the aspect ratio AR (AR=H/D) is 1. The idrofoil shape is a modified version of NACA0018 obtained warping the profile from the mid-chord such that the camber line fits the circular blade path (Fig. 1). The chord (c) of the modified cambered section is 32 mm length, corresponding to a solidity σ ($\sigma=cB/\pi D$, where B is the number of blades) of 17.5%. We chosen these data since blade profile and thickness are quite common, moreover other data series are available for a wide range of σ in tunnel [11] and for a full scale turbine with the same σ in open sea [12]. The water speed (U_∞) is 2.8 m/s; the corresponding Re_C ($Re_C=\rho c\Omega D/2\mu$, where ρ is the water density, Ω is the turbine angular velocity and μ is the dynamic viscosity) is 179000 at tip-speed-ratio TSR (TSR=$D\Omega/2U_\infty$,) of 2. Ansys FLUENT v.15 is adopted. Turbulence is modeled by the k-ω SST model that is common for vertical axis turbines since, thanks to its aptitude in cases involving high adverse pressure gradients and therefore smooth surface separations, it is able to simulate in more detail the vortices seen during dynamic stall at low TSR than the k–ω and k–ε models [13]. Grids are unstructured with the adding of regular quad element layers all around the walls to predict the boundary layer). The

wall distance from the first layer of cells is set to keep y+ low enough to capture flow separation phenomena. For the validation task the maximum y+ is 0.42 and the mean is 0.16, whereas for the simulations described in the following chapter the maximum y+ is 1.05 and the mean is 0.39. To simulate the turbine operating in conditions as similar as possible to the real conditions inside the water tunnel, the same width of the test-section is adopted for the computational domain in order to take into account for the horizontal solid blockage. Yet a longer domain is chosen in upstream to allow a non-uniform and realistic velocity profile before the rotor, since the only data know is the mean flow speed based on the flow rate elaborated by the pump. The domain length in downstream is set to allow a full development of the wake, avoiding numerical problems at the outlet boundary. As done by Ferreira for wind tunnel tests [14], inlet and outlet are placed 10D upwind and 14D downwind with respect to the rotor.

Fig.1 shows a comparison between calculated and experimental coefficient of power C_P ($C_P = P/0.5\rho HDU_\infty^3$, where P is the power generated) versus TSR. The high experimental and numerical C_P can be justify by the high blockage ratio (frontal turbine area / test-section area = 0.35) that increases the speed of the flow approaching the turbine. Despite of significant differences between predicted and experimental C_P (also found in [10]), some similarities in the trends of the C_P-TSR curves are seen, at least for TSR > 1.5, and the optimal TSR is matched. However, it should be noted that 2D simulations cannot give global performance (as C_P) really close to experimental results, especially in case of low AR, since it cannot consider blade tip losses and other physical mechanisms (in this case, the vertical blockage of the water tunnel) that would require a 3D approach.
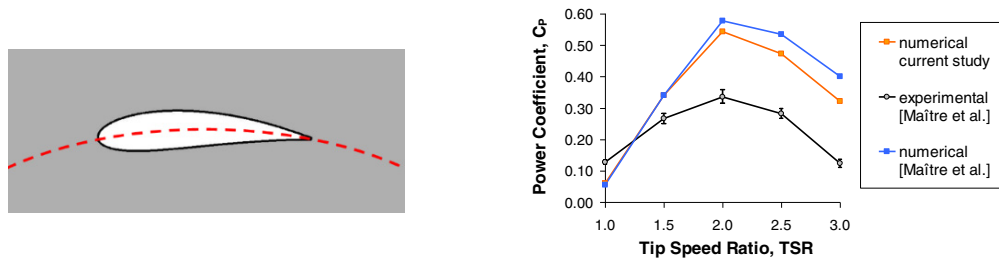

Fig. 1. (left) Blade path (red dashed line) and blade profile of the warped NACA0018; (right) comparison between experimental performance [10] and 2D CFD predictions obtained for the turbine in water tunnel.

3. Physical mechanisms of the interactions

The same turbine adopted for the validation was chosen (NACA0018, warped on the circumferential blade path; σ=17.5%), but the diameter is larger (D=1.0m) to raise Re_C to practical use values. Since we are interested in predict the behavior of a small farm of closely spaced turbines in similar operating conditions to those found offshore (open field conditions), the positions of inlet and lateral boundaries need to be far enough for the flow to be considered unbounded. The position of the outlet boundary must allow a complete wake development. On the base of preliminary simulations of the sensitivity to the domain dimensions, the size of the computational domain was set 55D along the x-coordinate (36D in upstream, 19D in downstream), and 48D along the y-coordinate. Most of the grid elements are located in the rotating domain (132000 cells for each turbine), around the turbines and in the near-wake; the total cell number is 253000 in case of single turbine, 618000 for 3-VATT arrangements. We simulate 25 revolutions: for the first 15 rev. a time-step corresponding to 1° of turbine rotation is used; for the successive 10 revolutions a finer time-step corresponding to 0.5° is used. Water speed is set 1.5 m/s, a value that could reasonably be representative of time-averaged speeds of tidal currents exploitable for power production. With c=183 mm, at TSR=1.75 Re_C=480000. From preliminary calculations the optimal TSR for an isolated turbine was 1.7, whereas in case of pairs of counter-rotating turbines it was 1.8. Thus in this chapter we adopt TSR=1.8 to better visualize and explain performance differences. Fig. 2 allows a qualitative comparison between an isolated and 3 side-by-side VATT in terms of streamlines and flow velocity, for a distance between the axes of adjacent rotors of 1.5D. The turbines belonging to the arrangement are two-by-two counter rotating: we name "A" the pair-layout that imply

blades spinning in the same water-flow direction at the layout inner side; we name "B" the pair-layout that imply blades spinning in the opposite direction to the water at the layout inner side. Because of the rotation verse, the wakes of a pair-A should slightly diverge in the lateral (y) direction whereas the wakes of a pair-B should slightly converge. In fact, as it happens in much greater extent for a flow past a rotating cylinder, the flow field downstream of a vertical axis turbine is asymmetric with a tendency to turn in the direction of rotation. However the turbine is partially permeable to the oncoming flow and thus the wake bending is just of few degrees (almost imperceptible).
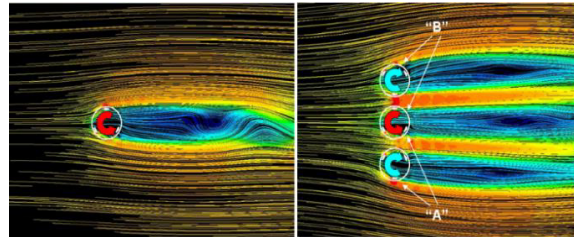

Fig. 2. Streamlines coloured with field velocity magnitude [range of the colour map 0÷2 m/s] and rotation verse for the isolated turbine (left) and for the side-by-side 3-turbine arrangement (right); A and B definition for the lower and the upper counter-rotating pairs.

Three phenomena are noticeable in Fig. 2: (1) the turbine **blockage** entails flow acceleration outside of the turbine(s) and, for the 3-VATT arrangement, inside the narrow aisles between the turbines; (2) the streamlines approaching the turbines at the inner sides of the arrangement (inner sides of pairs A and B) are constrained parallel to the x-direction (**flow x-alignment**), whereas for an isolated turbine the flow diverges at the sides; (3) a **wake contraction** is seen at the inner sides of the arrangement (particularly noticeable for the wake of the central turbine).

The blade angular position is defined by θ; independently of the rotation verse (anticlockwise or clockwise) the upwind path (0 ⩽ θ ⩽ 180) begins with the blade chord aligned to the current, the downwind path covers the range 180 ⩽ θ ⩽ 360. We start the analysis by observing what happens during upwind at the inner sides of the arrangement. In Fig. 3 (left) a comparison between the isolated turbine and the central turbine of the arrangement is depicted for a blade at θ=50°, thus during early upwind. It can be seen that the flow approaching the blade belonging to the arrangement is characterized by a lower value of the absolute speed (the arrangement offers a higher resistance to the incoming flow), but also by a direction more longitudinal that overcomes the above disadvantage resulting in a higher flow incidence on the blade (higher attack angle between the apparent velocity and the chord direction); as a consequence more torque is generated as also indicated by the pressure difference between the two sides of the blade and by the location of the stagnation point.
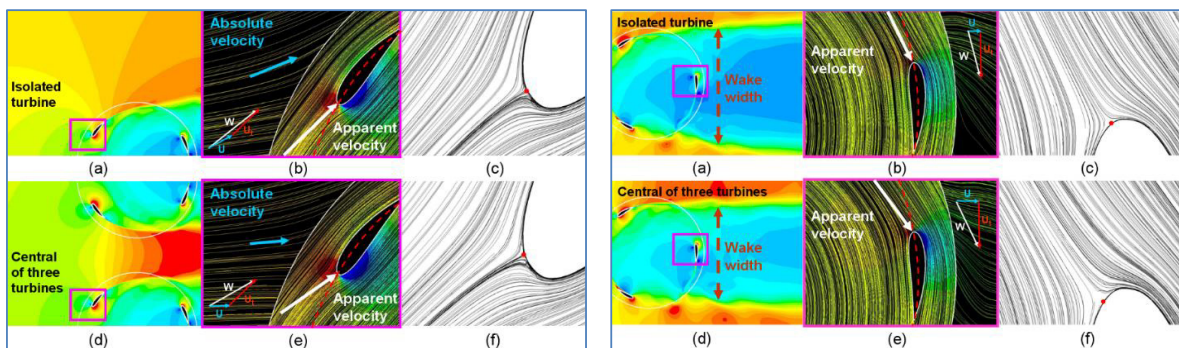

Fig. 3. Flow field comparison of an isolated turbine and the central turbine of a side-by-side layout during early upwind (left) and during downwind (right): (a, b) velocity map [0÷2 m/s]; (b, e) absolute and apparent streamlines coloured by pressure [-5000÷3000 Pa] with velocity vectors (U is the absolute flow velocity, U_t is the blade velocity, W is the apparent flow velocity); (c, f) stagnation point at the blade leading edge.

This mechanism (x-alignment of the flow approaching the blade) occurs at all the configuration inner sides: at the beginning of upwind for the upper rotor (layout B), at the end of upwind for the lower rotor (layout A), throughout the upwind for the central turbine of the arrangement. The one-blade instantaneous C_P for the turbines of the arrangement in comparison to an isolated turbine is shown in Fig. 4: torque production starts early for the upper turbine, lasts longer for the lower, both the events for the central.
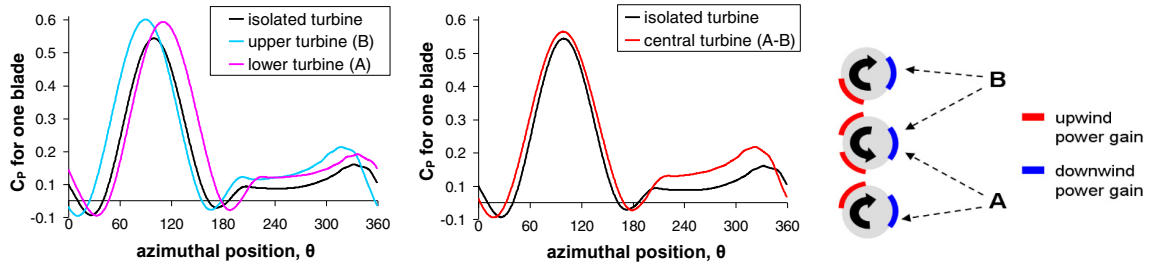

Fig. 4. (left and centre) One-blade instantaneous C_P in one revolution for the three turbines of the side-by-side layout in comparison to an isolated turbine (TSR=1.8); (right) angular ranges in upwind and downwind where power gain occurs.

We continue by observing what happens during downwind. In Fig. 3 (right) a comparison between the isolated turbine and the central turbine of the arrangement is depicted for a blade at θ=270°, thus at halfway of downwind. At this angular position the absolute flow direction is longitudinal for both the cases, thus it cannot make the difference. The flow approaching the blade belonging to the arrangement has a significantly higher velocity magnitude, due to the wake contraction induced by the close proximity of the upper and lower turbines. The increasing in flow speed is responsible for both a higher attack angle and a higher apparent velocity magnitude, and consequently for a higher torque production in downwind. This occurs for all the turbines of the layout and especially for the central turbine which wake is constrained at both its sides. C_P normalized by the maximum C_P achieved by the isolated turbine is 1.25 for the upper turbine, 1.26 for the central, 1.23 for the lower, resulting in a mean normalized C_P for the overall arrangement of 1.246. It is worth noticing that: the key mechanisms for the performance enhancing in upwind (x-alignment of the incoming flow) and in downwind (wake contraction) are the same observed for pairs of vertical axis wind turbines (Zanforlin and Nishino, [9]); the same mechanisms have been found increasing the power of a vertical axis wind turbine inserted in the throat of a convergent-divergent diffuser (Zanforlin and Letizia, [15]).

Afterwards we analyzed the behavior of 3 VATT set at the vertices of an equilateral triangle (distance between axes = 4.6D) and rotating at TSR=1.7. Streamlines and flow velocity magnitude are depicted in Fig. 5.
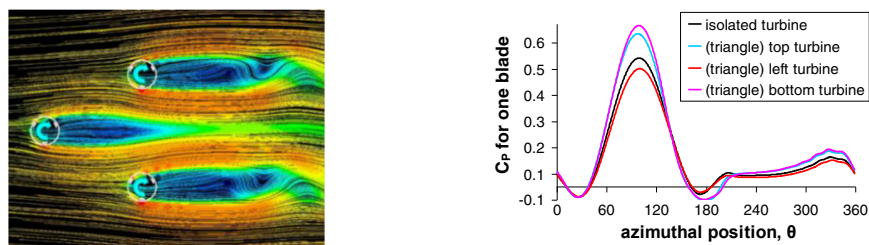

Fig. 5. (left) Streamlines coloured with velocity magnitude [range of the colour map 0÷2 m/s for the triangular layout; (right) one-blade instantaneous C_P for the three turbines of the triangular layout in comparison to an isolated turbine (TSR=1.7).

For the triangular layout an overall gain is found (less than half of the gain found for the side-by-side layout), however the downstream turbines registered a performance improvement but the upstream registered a loss. Gain and loss can be explained as blockage effects. In fact, the blockage generated by the upstream turbine address the

flow laterally, towards the downstream turbines that elaborate a higher flow rate, producing more torque, as shown in the instantaneous C_P graph of Fig. 5. On the other hand, the blockage from the downstream turbines prevents the complete development of the wake of the upstream turbine, reducing the flow rate elaborated by it, and therefore its power. By comparing the instantaneous C_P of Fig. 4 and 5, neither the effects of x-alignment (extension of the angular range producing torque in upwind) nor the effects of wake contraction (significant torque increasing in downwind) are seen for the triangular arrangement. We conclude that, how observed for staggered pairs of vertical axis wind turbines [9], effective x-alignment and wake contraction only occur in case of side-by-side arrangements.

4. Prediction of the energy output for a real case

To harvesting power from marine currents efficiently the flow speed needs to be higher than 1.0 m/s. Channels or constrictions between islands provide some of the best sites, as the flow is fast and rectilinear. One of the most potentially promising sites in the Mediterranean sea is the Strait of Messina, since there are locations in which measured current speeds exceed 2m/s. The currents inside the Strait are originated by tides and by steady currents oriented from the Tyrrhenian towards the Ionian Sea. The period of tidal currents is governed by the relative motion of the sun, the moon and the earth, and is about 12 hours 25 min. Tidal current speed varies with the time in a sinusoidal form, and the flow direction inverts in about every 6 hours. However, the current direction never inverts by exactly 180°, especially near the coasts of islands and isthmuses, therefore care is needed in choosing the arrangement of a VATT farm since if turbines are too much close the downstream turbines can be curtained by the upstream ones, depending on the current direction, with detriment of the overall power generated.

In this section we compare the energy output from a farm of 3 VATT arranged in two layout: side-by-side and triangular. In the former, turbines are two-by-two counter-rotating, TSR=1.75, distance between axes 2.3D. In the later, turbines are co-rotating, TSR=1.7, distance between axes 4.6D (as in Fig. 5). We now define two normalized power coefficients for the generic turbine belonging to the layout (k_i) and for the overall layout (K):

$$k_i = C_{P,i}/C_{P,\,isol}$$

$$K = \frac{1}{N}\sum_{i=1}^{N} k_i$$

where the subscripts "i" and "isol" respectively identify the turbine belonging to the arrangement and the isolated turbine, and N is the number of turbines belonging to an arrangement. First, setting a current speed of 1.5m/s, K are predicted by CFD for the two layout every 15° of current direction (φ). Results are shown in Fig. 6 and, due to geometrical properties, it periodically repeat every 180° for the side-by-side and every 120° for the triangular layout. The hydrodynamic interactions between turbines seems better exploited by the side-by-side layout than the triangular since the maximum K is higher (1.205 vs. 1.085) and the range of φ entailing K>1 is wider (120° vs. 36°).
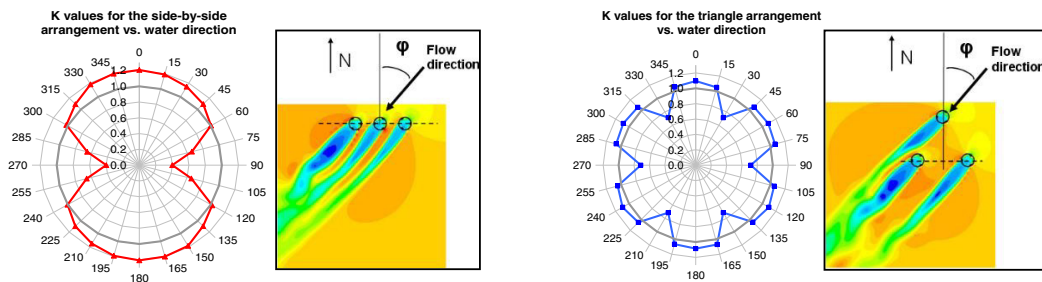

Fig. 6. Normalised power coefficient (K) versus water direction (φ) for the side-by-side (left) and for the triangular (right) layout; water current direction is defined in the lateral pane with respect to the turbine axis positions (in the examples φ = 45°).

On the other hand, significant efficiency losses occur for flow directions implying the wake of the upstream turbine cover one or both the downstream turbines (for instance, φ=90° and 270° for side-by-side layout). However, for both the layout, the sum of the φ-ranges giving K>1 are greater than the sum of the φ-ranges giving K<1.

These K-values were used to predict the energy output from the two layout during 28 days (a moon cycle) in a location in the Messina Strait close to Punta S. Ranieri. Current speed and direction were detected by Prof. Coiro of the University Federico II of Naples and his team using an Acoustic Doppler Current Profiling [16]. The graphs of current speed distribution and frequency of directions (Fig. 7) show some evidences: two main directions exist, 280° and 146° from North; the former direction is significant for energy production, since it is characterized by high frequency and reasonable current speeds; the later is less relevant due to high dispersion of the values (low frequencies) and to low speeds; the current inversion is not perfect, since the angular distance between the main directions is less than 180°. The power production from the isolated turbine is described by the ideal power curve of Fig. 7 (despite it would require a load control strategy unpractical for VATT). This curve is obtained by setting cut-in speed at 0.5m/s and nominal speed at 2.0m/s, and connecting with a cubic law the powers achieved with the C_P predicted from CFD at 0.5m/s and 2.0m/s, purged by 30% to take into account for losses.
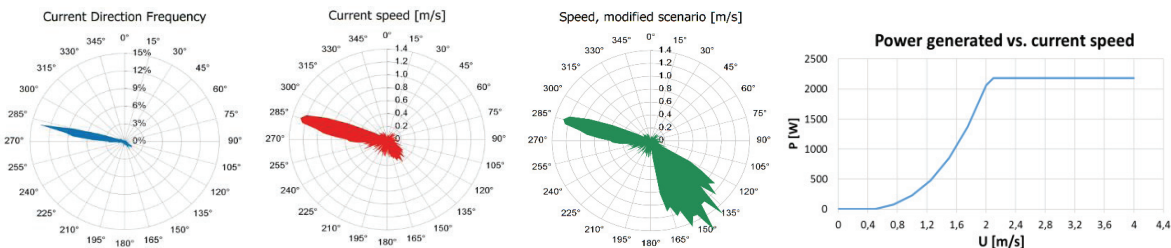

Fig. 7. From left to right: current direction frequencies; current speed distribution for the original scenario; current speed distribution for the modified scenario; simple power curve adopted for the isolated turbine.
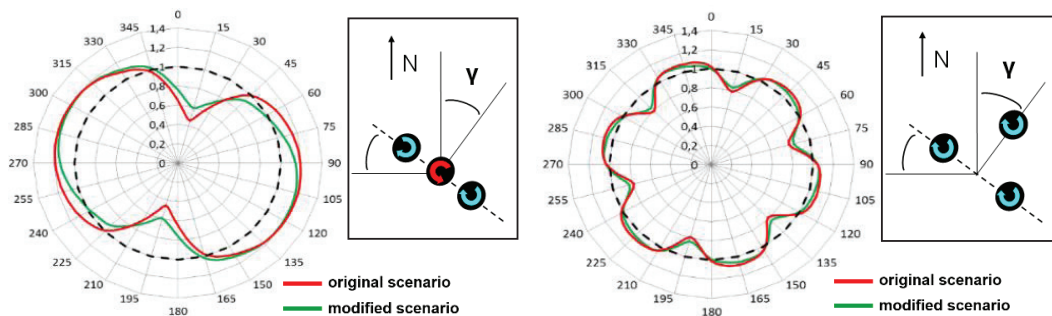

Fig. 8. Normalized energy output in a moon cycle (i.e., energy divided by the energy from 3 isolated turbines) in case of the original and of the modified scenarios for the side-by-side (left) and for the triangular layout (right) versus the angular orientation of the arrangement (γ).

Finally, Fig. 8 shows the layout normalized output (energy produced by the layout divided by the energy output of 3 isolated VATT) versus the geographical setting of the arrangement, calculated by multiply the power-curve of an isolated turbine by the K values found with CFD. The best setting of each layout is one that allows the maximum normalized output. Results for the original scenario are encouraging, giving maximum normalized output of 1.205 for the side-by-side and 1.085 for the triangular layout. However, most of the speeds around the 146° main direction are below the cut-in. To verify if the two arrangements would lead to energy output enhancing even if the current speeds around the two main directions were comparable, we hypothesized a new scenario (named "modified scenario") by multiply by 4.0 the original speeds with direction in a range of 51° centered on the 146° direction (see

Fig. 7). Results are still satisfactory and similar to the previous (the maximum normalized output is 1.19 for the side-by-side and 1.06 for the triangular layout), however no adjustments have been made to the frequencies of the increased speeds, thus the cumulative frequency giving energy (U_∞ > 0.5m/s) around the 146° main direction is significantly lower than the cumulative frequency giving energy around the 280° main direction (16.9% vs. 55.5%).

5. Conclusions

The CFD analysis of three VATT set in close proximity confirmed how found in a previous paper focused on pairs of counter-rotating wind turbines [9], proving that three main mechanisms can explain a performance increasing with respect to isolated turbines: (1) turbine lateral blockage that entails flow acceleration outside of the turbines (effect important for the downstream turbines belonging to a triangular layout) and inside the aisles between adjacent turbines; (2) flow x-alignment, that it is a consequence of blockage and allows higher attack angle during upwind; (3) wake contraction, that increases torque generation during downwind. Blockage is responsible for a moderate performance increasing exhibited by a triangular layout. Flow alignment and wake contraction only occur for side-by-side layout, and justify the superiority of this arrangement in terms of maximum normalized performance. Another advantage of side-by-side layout is the wide range of flow directions (about 120°) that allows a power gain on isolated turbines. This feature is expected to make side-by-side layout advantageously adoptable also in case of tidal currents characterized by dispersion of directions around the main directions or a non perfect inversion ever 6 hours, as it often happens in real cases. However, despite the encouraging predictions obtained for the location Punta S. Ranieri (Strait of Messina) and for a modified scenario, other series of experimental data would be needed to verify the performance advantages of the arrangements in a comprehensive variety of real scenarios.

References

[1] Bai G, Jun Li J, Fan P, Li G. Numerical investigations of the effects of different arrays on power extractions of horizontal axis tidal current turbines. Renewable Energy 53 (2013) 180-186.
[2] Gebreslassie M G, Tabor G R, Belmont M R. Investigation of the performance of a staggered configuration of tidal turbines using CFD. Renewable Energy, Volume 80, August 2015, Pages 690-698.
[3] Whittlesey R W, Liska S, Dabiri J O. Fish schooling as a basis for vertical axis wind turbine farm design. Bioinspiration & biomimetics, 2010, vol. 5
[4] Dabiri J. O, Potential order-of-magnitude enhancement of wind farm power density via counter-rotating vertical-axis wind turbine arrays. Journal of renewable and sustainable energy, 2011, vol. 3.
[5] Araya D B, Craig, A E, Kinzel M, Dabiri J O, "Low-order modeling of wind farm aerodynamics using leaky Rankine bodies", Journal of renewable and sustainable energy, 2014, vol. 6, 063118.
[6] Li Y, Calısal S M. Modeling of twin-turbine system swith vertical axis tidal current turbines: Part I-Power output. Ocean Engineering 37 (2010) 627-637.
[7] Feng G et al. Optimizing the Land Use for Wind Farms Using Vertical Axis Wind Turbines. PO.ID 192, Europe's premier wind energy conference and exhibition, European Wind Energy Association (EWEA), 2014, Barcelona, Spain.
[8] Giorgetti S, Pellegrini G, Zanforlin S. CFD investigation on the aerodynamic interferences between medium-solidity Darrieus vertical axis wind turbines, Energy Procedia, Volume 81, December 2015, Pages 227-239.
[9] Zanforlin S and Nishino T. Fluid dynamic mechanisms of enhanced power generation by closely spaced vertical axis wind turbines, Renewable Energy 99 (2016) 1213-1226.
[10] T. Maître T, Amet E, Pellone C. Modeling of the flow in a Darrieus water turbine: Wall grid refinement analysis and comparison with experiments. Renewable Energy 51 (2013) 497-512.
[11] Kiho S, Shiono M, Suzuki K. The power generation from tidal currents by Darrieus turbines. WREC 1996.
[12] Shiono M, Suzuki K, Kiho S. An Experimental Study of the Characteristics of a Darrieus Turbine for Tidal Power Generation. Electrical Engineering in Japan, Vol. 132, No. 3, 2000.
[13] Simao Ferreira CJ, Bijl H, van Bussel G, van Kuik G. Simulating dynamic stall in a 2D VAWT: modeling strategy, verification and validation with particle image velocimetry data, the Science of making torque from wind. J Phys Conf Ser 2007;75.
[14] Nobile R, Vahdati M, Barlow JF, Mewburn-Crook A. Unsteady flow simulation of a vertical axis augmented wind turbine: A two-dimensional study, J. Wind Eng. Ind. Aerodyn.125 (2014) 168–179.
[15] Zanforlin S, Letizia S. Improving the performance of wind turbines in urban environment by integrating the action of a diffuser with the aerodynamics of the rooftops, Energy Procedia Volume 82, December 2015, Pages 774–781.
[16] Coiro D and Troise D. Stima della produzione energetica da correnti marine nello Stretto di Messina. ENEA Report RdS/2012/172.